ELSEVIER

International Journal of Mass Spectrometry 194 (2000) 145–164

International Journal of Mass Spectrometry

Fragmentation reactions of all 64 protonated trimer oligodeoxynucleotides and 16 mixed base tetramer oligodeoxynucleotides via tandem mass spectrometry in an ion trap

Ana K. Vrkic[a], Richard A.J. O'Hair[a,*], Simon Foote[b], Gavin E. Reid[a,c]

[a]*School of Chemistry, University of Melbourne, Parkville, Victoria 3052, Australia*
[b]*The Walter and Eliza Hall Institute of Medical Research, P.O. Royal Melbourne Hospital, Parkville, Victoria 3050, Australia*
[c]*Joint Protein Structure Laboratory, The Ludwig Institute for Cancer Research and the Walter and Eliza Hall Institute of Medical Research, P.O. Royal Melbourne Hospital, Parkville, Victoria 3050, Australia*

Received 24 March 1999; accepted 29 June 1999

Abstract

The gas phase fragmentation reactions of the $[M + H]^+$ ions derived from all 64 trimer oligodeoxynucleotides and 16 isomeric tetramer oligodeoxynucleotides each containing adenine, thymine, guanine, and cytosine were examined by electrospray ionization using multistage tandem mass spectrometry in a quadrupole ion trap. The MS/MS and MS^3 spectra of the $[M + 2H]^{2+}$ ions of 16 isomeric tetramer oligodeoxynucleotides were also examined. The initial collisionally induced dissociation (CID) reaction mechanism for $[M + nH]^{n+}$ ions involves neutral base loss. The relative abundance of each of these neutral losses is dependent on the relative proton affinity (where $C \approx G > A \gg T$), and position within the oligodeoxynucleotide sequence ($5' > 3' >$ internal). These non-sequence $[M + H - B_nH]^+$ ions (where B_n denotes the nucleobase in the *n*th position from the 5′ position), provide information on the identity but not the position of the base. MS^3 experiments were carried out to demonstrate that these ions can provide further sequence information. It is proposed that intramolecular proton transfer following base loss leads to cleavage of the 3′ − C–O phosphodiester bond (relative to the site of base loss) to yield an ion-molecule complex, which then undergoes either proton transfer or direct dissociation to yield complementary w- and (a − B)-type ions. For the trimer oligodeoxynucleotides, loss of the 5′ base yields w_2^+-type ions, loss of the 3′ base yields results in neutral water loss with formation of $(a_3 - B_3)^+$-type ions and loss of the internal base yields w_1^+ and $(a_2 - B_2)^+$-type ions. The MS/MS and MS^3 spectra of the $[M + H]^+$ and $[M + 2H]^{2+}$ ions of 16 isomeric tetramers were examined and found to follow the trends observed for the trimers. (Int J Mass Spectrom 194 (2000) 145–164) © 2000 Elsevier Science B.V.

Keywords: Tandem mass spectrometry; Sequencing; Protonated oligonucleotides

1. Introduction

The extensive use of synthetic oligodeoxynucleotides in all facets of molecular biology has resulted in rising demand for characterization of this important class of compounds [1–3]. With the completion of the human genome project, an efficient and accurate method of mutation detection will be crucial in implicating disease candidate genes and in screening programs, which follow the identification of disease

* Corresponding author. E-mail: r.ohair@chemistry.unimelb.edu.au

This article is Part XVIII of the series "Gas Phase Ion Chemistry of Biomolecules."

Dedicated to Professor Jim Morrison on the occasion of his 75th birthday and in recognition of his important contributions to mass spectrometry.

1387-3806/00/$20.00 © 2000 Elsevier Science B.V. All rights reserved
PII S1387-3806(99)00150-5

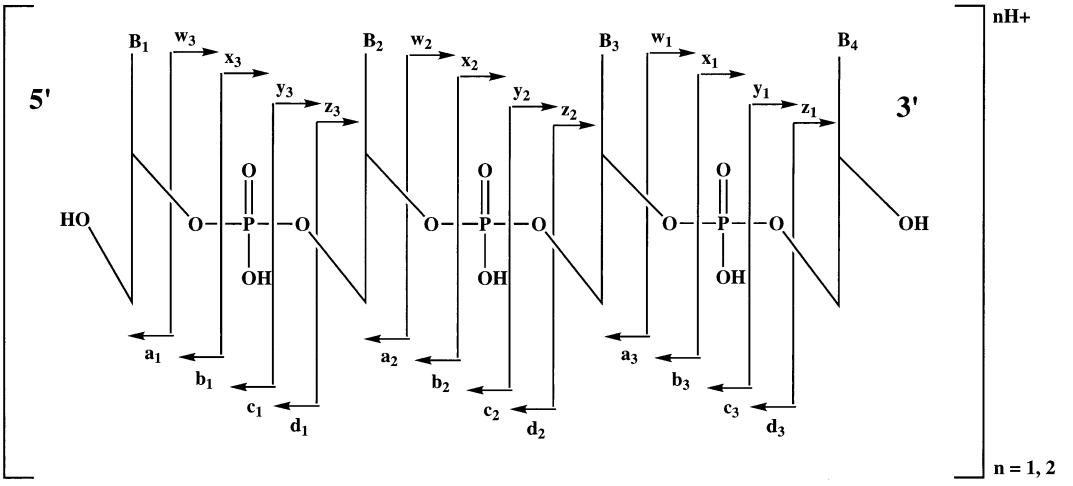

Scheme 1.

causing mutations. Techniques are therefore required for the rapid resequencing [4] of large regions of DNA to allow for the detection and identification of nucleotide mutations therein. Mass spectrometric based resequencing techniques may potentially provide the means of achieving the above mentioned requirements. Indeed, the potential for mass spectrometry to become a vital tool for solving problems involving peptide and oligodeoxynucleotide structures is due primarily to two significant capabilities: (a) it can be used to determine the molecular weight of a biomolecule, and (b) it can provide partial to complete sequence information [5]. When coupled with soft ionization techniques such as matrix-assisted laser desorption ionization (MALDI) and electrospray ionization (ESI) to allow the facile introduction of these molecules into the gaseous phase, sequence information can be rapidly obtained using tandem mass spectrometry (MS/MS) [e.g. collision-induced dissociation (CID)] of mass selected precursor ions. The recent development and commercialization of instruments such as ion traps allow further sequence information to be obtained by performing MS^3 experiments on mass selected product ions.

The site of ionization, and the charge polarity (anions versus cations) of oligodeoxynucleotides are all expected to play a key role in determining the major fragmentation processes observed. To date, most studies on the fragmentation reactions of oligodeoxynucleotides have focussed on $[M - nH]^{n-}$ ions [6–8]. Pioneering work by McLuckey and coworkers has resulted in the formation of a product ion nomenclature for anionic oligodeoxynucleotides [9]. This nomenclature can readily be adapted to suit cationic oligodeoxynucleotides (Scheme 1).

In comparison to $[M - nH]^{n-}$ ions, much less is known about the fragmentation behaviour of $[M + nH]^{n+}$ oligodeoxynucleotide cations. Previous limited studies have been performed using Fourier transform ion cyclotron resonance FTICR [10] and triple quadrupole mass spectrometers [11–14]. (Note that in each case, product ions resulting from fragmentations where the phosphate-sugar bonds are cleaved are termed "sequence" ions [15], whereas those resulting from fragmentations remote to the phosphate-sugar linkage (for example, base loss) are termed "non-sequence" ions).

Although the collision-induced dissociation pathways of all 16 possible dioligodeoxynucleotides have been comprehensively studied using FTICR mass spectrometry experiments by Beauchamp and coworkers [10], no account on the fragmentation reactions of trimers has been reported. Furthermore, the study of tetramer and larger oligodeoxynucleotide by MS/MS investigations have been restricted to only two triple quadrupole studies. The following general trends have emerged from these limited low energy

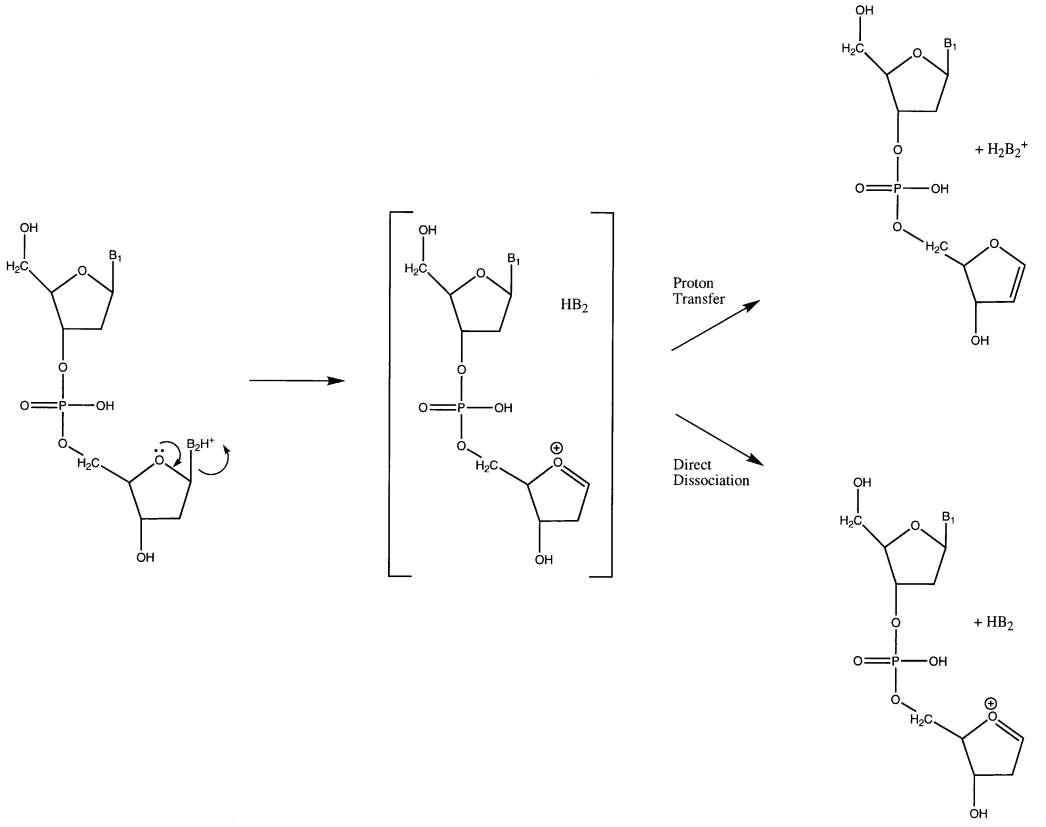

Scheme 2.

(<100 eV) CID MS/MS studies on $[M + nH]^{n+}$ ions derived from oligodeoxynucleotides: (i) the major fragmentation pathway is directed by the site of protonation leading to the "non-sequence" loss of a base, generally at the 3′ position for dioligodeoxynucleotides (Scheme 2) and at the 5′ position for tetramer oligodeoxynucleotides; (ii) the order of the base losses observed, C ≈ G > A ≫ T, generally agrees with the known proton affinities of these nucleobases; (iii) phosphodiester chain cleavage at the C–O bond with concomitant base loss yields w-type and a − B type "sequence" ions.

Given that (i) there has been a lack of ion trap MS/MS experiments performed on the $[M + nH]^{n+}$ ions of oligodeoxynucleotides, and (ii) limited work has been performed on examining the use of MS^3 experiments of product ions to obtain more complete sequence information (particularly from the initial major "non-sequence" product ions corresponding to base loss), we herein report the fragmentation behaviour of all 64 protonated trimers and 16 tetramer oligodeoxynucleotides using MS/MS and MS^3 on an ESI-ion trap mass spectrometer. Additionally, we examine the potential for MS^3 experiments to distinguish potentially isomeric "sequence" and "non-sequence" ions and propose detailed mechanisms for the formation of these "non-sequence" and "sequence" ions.

2. Experimental

2.1. Materials

All trimer and tetrameric oligodeoxynucleotides were purchased from Bresatec (Thebarton, SA, Australia) as crude deprotected salts. HPLC grade water was obtained from a MilliQ system. Ammonium

formate and formic acid were purchased from AJAX Chemicals (Auburn, NSW, Australia). HPLC grade methanol was obtained from Merck (Kilsyth, Victoria, Australia).

2.2. Purification of crude oligodeoxynucleotides

Oligodeoxynucleotides were fractionated by RP-HPLC using a Hewlett-Packard HP1050 liquid chromatograph. The column used in this study (Brownlee RP-300, 7 μm, 100 mm $\times$ 2.1 mm i.d.) was obtained from Perkin Elmer (Norwalk, CT, USA). Trimer samples (15 μg) and tetramer samples (20 μg) were dissolved in 200 μL of water, then loaded onto the column at 1 mL/min (at 0% B) and eluted at 0.2 mL/min over a linear 10 min gradient from 0–50% B, where solvent A was 50 mM ammonium formate pH 5.4 and solvent B was methanol. The column was operated at 45 °C and the eluent was monitored by UV absorbance at 254 nm. The fractions, which were collected manually, were frozen prior to direct MS analysis as described below.

2.3. Mass spectrometry

Protonated $[M + H]^+$ ions were formed via electrospray ionization (ESI) on a Finnigan model LCQ (San Jose, CA) quadrupole ion trap mass spectrometer. The purified samples ($\sim$100 μL) obtained from the HPLC were introduced to the mass spectrometer at 3 μL/min (using a Harvard syringe drive) via a length of 190 μm o.d. $\times$ 50 μm i.d. fused silica tubing. The spray voltage was set at -5 kV. Nitrogen sheath gas was obtained from a boiling liquid nitrogen source supplied at 30 1b/in.^{2}. The heated capillary temperature was 200°C. MS/MS and MS^3 experiments were performed on mass selected ions in the quadrupole ion trap mass spectrometer using standard isolation and excitation procedures with a collision energy between 15 and 20%. The mass spectrometer was further tuned for the singly and doubly charged ions of the tetramer oligodeoxynucleotides in order to optimise their yields. All data collected were the average of 10 scans.

3. Results and discussion

In order to ensure accurate and sensitive analysis of oligodeoxynucleotides, cations such as sodium and potassium must be removed prior to analysis by mass spectrometry [16]. The most generally applicable and readily available form of desalting oligodeoxynucleotides is via reversed-phase high-performance liquid chromatography (RP-HPLC). Thus, in this study, each of the 64 trimer and 16 tetramer oligodeoxynucleotides were desalted via RP-HPLC using an ammonium formate/methanol gradient system. Following this desalting procedure, cation adduction to the oligodeoxynucleotides in the gas phase was found to be significantly suppressed.

3.1. Tandem mass spectrometry on the $[M + H]^+$ ions of all 64 trimer oligodeoxynucleotides

Tandem mass spectrometric experiments were performed on all of the singly charged protonated trimer oligodeoxynucleotides produced via electrospray ionization. In keeping with previous studies [10–14], it was found that ions corresponding to neutral base loss were observed as the major products. However, in contrast to previous findings where 3′ base loss was primarily observed, comparison of the base loss abundances for each of the 64 trimer oligodeoxynucleotides studied here (Table 1) established a different pathway. The major reaction pathway generally involves loss of a neutral base from the 5′ terminus when C and G are in that position, only sometimes when A is in that position (i.e. when C and G are not in the 3′ position), and not for T. The relative order of base loss abundances was found to be C $\approx$ G $>$ A $\gg$ T. This observation correlates with the known proton affinites of the bases and their stable tautomers as discussed below. Exceptions to this general rule were observed when thymine was present at the 5′ terminus where neutral base loss from either the 3′ or internal position occurred (the relatively high abundance of TH loss for ATC is the only anomolous result). The relative ion abundances for base loss at these sites was in accordance with the order of base losses observed at the 5′ position (i.e. in the order C $\approx$ G $>$ A $\gg$ T).

Table 1
LCQ CID MS/MS of the $[M + H]^+$ ions of all 64 trimer oligonucleotides

Sample	d($B_1B_2B_3$) (*m/z*)	Product ions[d] (% relative abundance)						
		−AH	−GH	−CH	−TH	w_1^+	w_2^+	$(a_2 - B_2)^+$
1	AAA (878)[a]	100	—	—	—	2	56	2
2	AAG (894)[a]	69	39	—	—	1	100	3
3	AAC (854)	35	—	100	—	1	21	1
4	AAT (869)[a]	100	—	—	1	—	53	3
5	AGA (894)	100	18	—	—	6	60	2
6	AGG (910)	46	100	—	—	3	50	4
7	AGC (870)	46	13	100	—	1	18	2
8	AGT (885)	100	35	—	1	1	49	12
9	ACA (854)[a]	100	—	37	—	5	44	4
10	ACG (870)	93	100	92	—	4	72	2
11	ACC (830)	21	—	100	—	—	6	—
12	ACT (845)	63	—	100	1	—	74	30
13	ATA (869)	100	—	—	1	—	39	—
14	ATG (885)	56	50	—	1	—	100	—
15	ATC (845)	23	—	100	16	—	8	—
16	ATT (860)	4	—	—	1	—	100	—
17	GAA (894)	6	100	—	—	1	39	1
18	GAG (910)	—	100	—	—	—	32	—
19	GAC (870)[a]	—	100	32	—	—	60	—
20	GAT (885)	1	100	—	1	—	31	1
21	GGA (910)	1	100	—	—	1	33	1
22	GGG (926)	—	100	—	—	—	16	—
23	GGC (886)	—	100	16	—	—	25	—
24	GGT (901)	—	100	—	—	—	14	—
25	GCA (870)	9	100	29	—	1	61	1
26	GCG (886)	—	100	10	—	1	36	1
27	GCC (846)	—	100	36	—	—	43	—
28	GCT (861)	—	100	23	1	—	97	4
29	GTA (885)	3	100	—	1	—	36	—
30	GTG (901)	—	100	—	—	—	27	—
31	GTC (861)	—	100	74	—	—	84	—
32	GTT (876)	—	32	—	1	—	100	—
33	CAA (854)[a]	31	—	100	—	1	65	—
34	CAG (870)	7	49	100	—	1	67	1
35	CAC (830)	3	—	100	—	—	24	—
36	CAT (845)	2	—	100	1	—	26	1
37	CGA (870)	2	4	100	—	1	33	1
38	CGG (886)	—	42	100	—	1	47	—
39	CGC (846)	—	5	100	—	1	28	1
40	CGT (861)	—	4	100	1	—	33	—
41	CCA (830)	9	—	100	—	2	17	1
42	CCG (846)	—	45	100	—	1	34	1
43	CCC (806)	—	—	100	—	1	15	2
44	CCT (821)	—	—	100	1	—	42	5
45	CTA (845)	3	—	100	—	1	31	—
46	CTG (861)	—	20	100	—	—	69	—
47	CTC (821)	—	—	100	—	—	19	—
48	CTT (836)	—	—	10	—	—	100	—
49	TAA (869)[a]	100	—	—	1	23	12	—
50	TAG (885)[a]	31	100	—	1	4	4	—
51	TAC (845)	6	—	100	1	1	2	—

(*continued*)

Table 1 (*continued*)

Sample	d($B_1B_2B_3$) (*m/z*)	Product ions[d] (% relative abundance)						
		−AH	−GH	−CH	−TH	w_1^+	w_2^+	$(a_2 - B_2)^+$
52	TAT (860)[a,b]	86	—	—	12	16	62	38
53	TGA (885)	16	100	—	2	36	2	—
54	TGG (901)	—	100	—	1	7	1	—
55	TGC (861)	—	41	100	—	2	1	—
56	TGT (876)[a]	—	100	—	4	8	—	30
57	TCA (845)	14	—	100	1	13	2	—
58	TCG (861)	—	67	100	1	16	2	—
59	TCC (821)	—	—	100	1	1	1	—
60	TCT (836)[a]	—	—	100	1	2	4	29
61	TTA (860)	11	—	—	5	2	32	100
62	TTG (876)	—	24	—	3	—	3	38
63	TTC (836)	—	—	24	—	—	—	24
64	TTT (851)[c]	—	—	—	4	—	44	3

[a] z_2^+ ion greater than 10%.
[b] The base peak is due to the formation of an ion at *m/z* 305, which could be either of the isomer c_3 or x_1 sequence ions.
[c] The base peak is due to the formation of the z_2^+ ion at 528.9.
[d] Only those ions greater than or equal to 1% relative abundance are shown.

In contrast to our findings that base loss preferentially occurs from the 5′–terminus, previous work done on dideoxynucleotides suggests that base loss occurs via the 3′–terminus. An important factor that must be taken into account when comparing these two systems is that the dideoxynucleotides contain no internal residue and do not, therefore, take into account what effect an internal residue may have on a system.

Assuming that the fragmentation reactions of protonated oligodeoxynucleotides are charge directed, it is clear that the site of protonation on the nucleobase has a major influence on the likelyhood of fragmentation via nucleobase loss. This is due to two main reasons: (i) protonation either labilizes or strengthens adjacent bonds, which determines which bonds will break [17], (ii) protonation converts the nucleobase into a neutral leaving group, whose tautomeric structure and stability will vary depending upon the initial site of protonation. Thus, the most thermodynamically favoured site of protonation may neither result in ready fragmentation nor yield the best leaving group. These points are discussed further below using Scheme 3 and data from Table 2.

Unfortunately, there is a dearth of information on the proton affinities of oligodeoxynucleotides, so we need to turn to smaller model systems to gain insights into the relative proton affinities of their constituents. Thus, Table 2 depicts both the theoretical and experimental proton affinity values for the nucleic acid bases, their respective nucleosides, and a model for the phosphate backbone, along with the relative energies of the tautomeric structures of the leaving groups. Upon examination of the theoretical proton affinity values for the nucleic acid bases [18,19], the preferred sites of protonation are shown to be at N_3 for cytosine, N_7 for guanine, N_1 for adenine, and O_4 for thymine. Additionally, the experimental proton affinity values [20,21] appear to be consistent for each nucleic acid base, suggesting an overall order of C ≈ G > A ≫ T. Looking at the nucleosides, the theoretically preferred sites of protonation are shown to be dG4, dT3, dU3, dC1, dC2, dA1, and dA2 (Scheme 3) at differing levels of theory [22,23]. Both the experimental and theoretical proton affinities for the nucleosides indicate that dG ≈ dA > dC ≫ dT. The theoretical studies have pointed out that the precise ordering of the proton affinities of C, G, and A and dC, dG, and dA are complicated by the fact that there are multiple neutral tautomers to be considered (some of which have similar energies) and that each of these different neutral tautomers contains multiple protonation sites. Nonetheless, it can be definitively concluded that C,

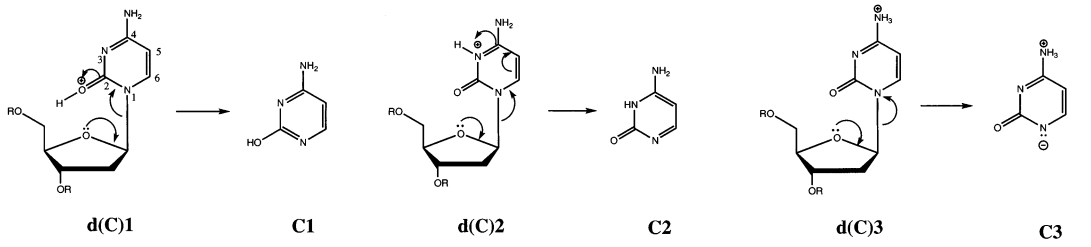

Scheme 3 (a)

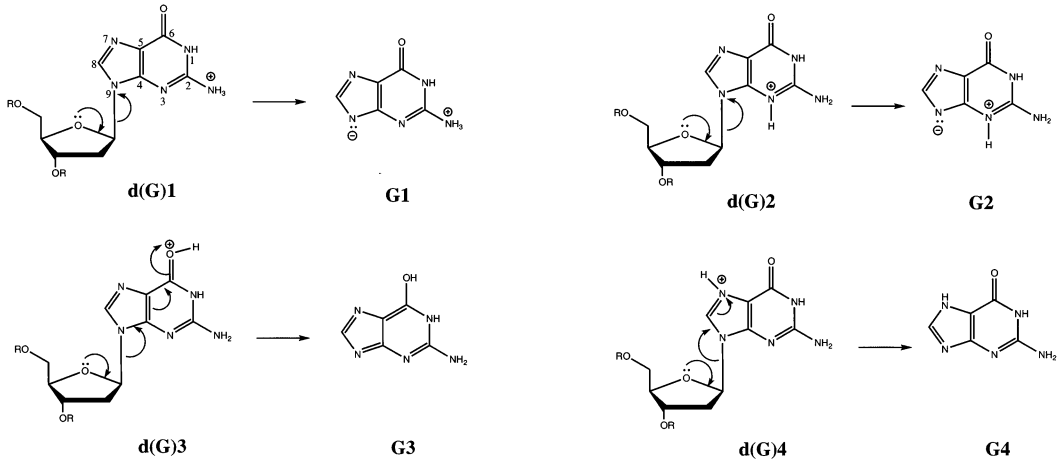

Scheme 3 (b)

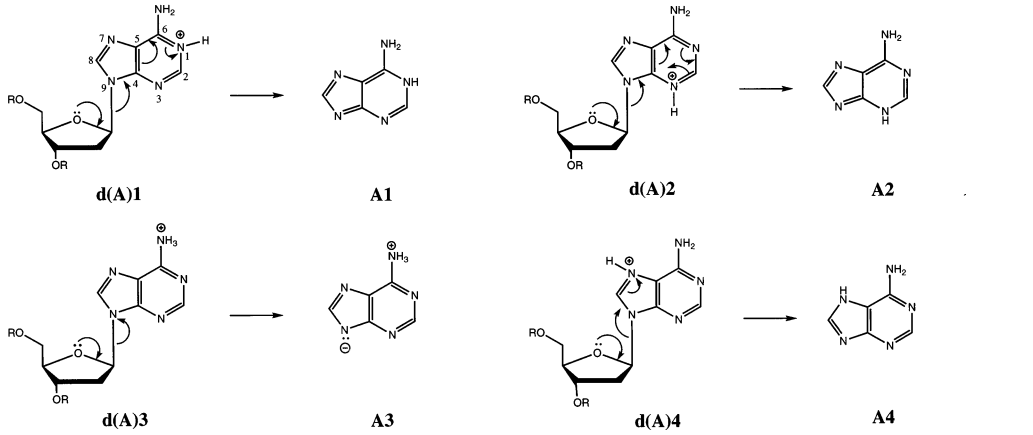

Scheme 3 (c)

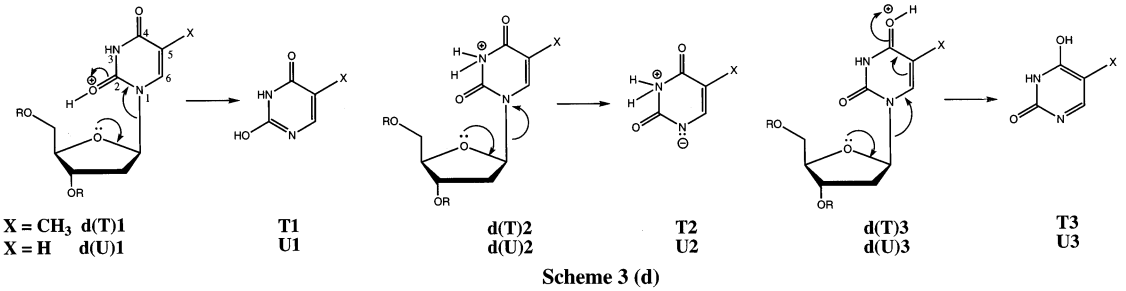

Scheme 3 (d)

Scheme 3.

Table 2
Experimental and theoretical proton affinities of nucleobases and nucleosides and neutral tautomer energies of nucleobases

Nucleobase	P.A. (theoretical) (kcal/mol)	P.A. (experimental) (kcal/mol)	Nucleoside	P.A. (theoretical) (kcal/mol)	P.A. (experimental) (kcal/mol)	Leaving group (kcal/mol)[a]
C	O_2 228.3[b]			dC1 226.4[f]		
	241.7[c]	227.0[d]	dC	234.9[g]	236.2[d]	C1 3.8
		225.9[e]		dC2 230.2[f]	233.2[e]	C2 7.1
	N_3 229.1[b]			233.7[g]		C3 [h]
	249.2[c]			dC3 204.9[g]		
G	N_3 228.5[c]			dG1 196.7[g]		
				dG2 217.8[f]		G1 [h]
	O_6 223.8[b]	229.3[d]	dG	216.8[g]	237.9[d]	G2 [h]
	233.1[c]	227.4[e]		dG3 219.6[f]	234.4[e]	G3 31.8
				227.3[g]		G4 2.5
	N_7 230.3[b]			dG4 226.5[f]		
	244.7[c]			234.4[g]		
A	N_1 225.8[b]			dA1 224.2[f]		
	241.1[c]			229.8[g]		A1 26.5
	N_3 223.6[b]	225.3[d]	dA	dA2 228.8[f]	237.0[d]	A2 14.2
	240.0[c]	224.2[e]		227.4[g]	233.6[e]	A3 [h]
	N_7 218.2[b]			dA3 210.3[g]		A4 11.0
	232.1[c]			dA4 218.1[f]		
				223.2[g]		
T	O_2 199.9[b]			dT1 202.9[f]		T1 17.0
	204.4[c]			dU1 203.3[g]	226.7[d]	U1 17.2
		210.5[d]	dT		224.9[e]	T2 [h]
	O_4 208.8[b]	209.0[e]		dT3 209.6[f]	208.6[d]	U2 [h]
	211.8[c]			dU3 213.1[g]		T3 32.6
						U3 28.6
$(CH_3O)_3PO$	212.9[d]					

[a] Relative energies of the various tautomers of the neutral nucleobase leaving groups are taken from [24] and [25].
[b] [18].
[c] [19].
[d] [20].
[e] [21].
[f] [22].
[g] [23].
[h] The leaving group is a zwitterion and is expected to have a high energy in the gas phase.

G, and A and dC, dG, and dA are much more likely to be protonated compared to T and dT, which consistently have lower proton affinites.

Turning to the relative energies of the tautomeric forms of the leaving groups, it is clear that the most stable forms considered here are C1, G4, A4, T1, and U1 [24,25]. Furthermore, C3, G1, G2, A3, T2, and U2 are all expected to be poor leaving groups in the gas phase as they are zwitterions. Comparing the proton affinities of both the nucleosides and their leaving groups it can be concluded that the preferred site of protonation does not always give the most stable tautomeric form of leaving group.

Therefore, the order of base loss for the 64 trimer oligodeoxynucleotides studied here (C $\approx$ G $>$ A $\gg$ T), generally follows the trends based upon the predicted and experimentally determined proton affinities and leaving group structures (i.e. tautomers) of each of the nucleic acid bases, suggesting that protonation of the base leads to base loss at that position.

A further complication is that base loss from a protonated deoxyribose nucleotide can occur via two

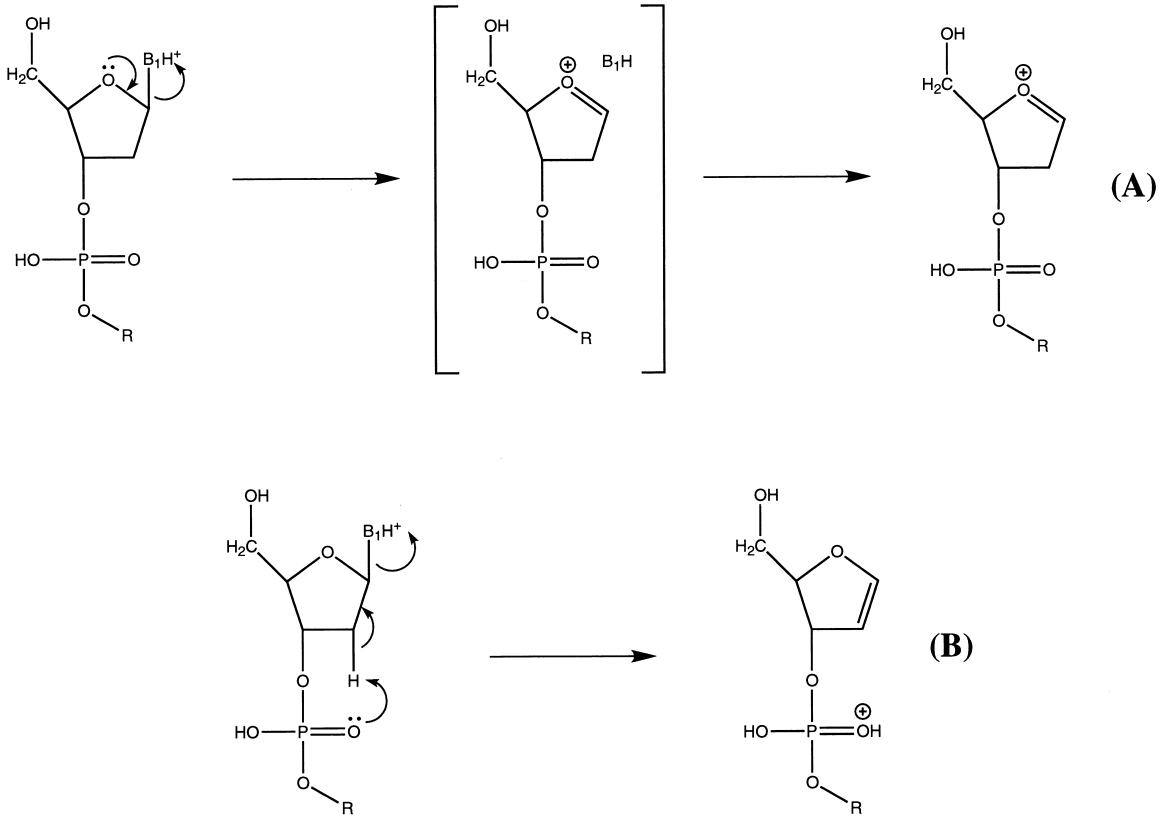

Scheme 4.

different possible pathways (Scheme 4). The first mechanism involves loss of the base via an E1 reaction, a two step process in, which a carbocation intermediate is formed followed by loss of a neutral base to form the oxonium ion (A). The second mechanism involves loss of the base via an intramolecular E2 single step reaction, in which a furan double bond (B) forms at the same time as the base is leaving. Note that the ions formed via both the E1 and E2 mechanisms are isomeric and because the mass spectrometer only measures the mass-to-charge ratio, it would be difficult to distinguish between these two ions.

Clearly, the choice of pathway (i.e. E1 versus E2) for base loss relies upon the position of the base within the deoxyribose nucleotide. 3′ base loss can only occur via the E1 mechanism (Scheme 4A) as nucleophilic attack from the 3′-phosphate oxygen is required for the E2 mechanism (Scheme 4B) to occur. 5′ or internal base loss however, could conceivably occur via either the E1 or E2 mechanisms. Note that intramolecular proton transfer to the phosphate oxygen following 5′ or internal base loss via the E1 mechanism could lead to formation of the same isomer as generated from the E2 mechanism.

In addition to neutral base loss, less abundant product ions corresponding to phosphodiester chain cleavage at the C–O bond yielding w- and (a − B)-type "sequence" ions were observed. Generally, the w_2^+ ion was observed as the most abundant sequence ion, with the w_1^+ and $(a_2 - B_2)^+$ ions present in significantly lower abundances. When thymine was present at the 5′ position, however, the relative yields of the w_1^+ and $(a_2 - B_2)^+$ ions increased, while those of the w_2^+ ions decreased. Note that the nomenclature of the $(a_n - B_n)^+$-type se-

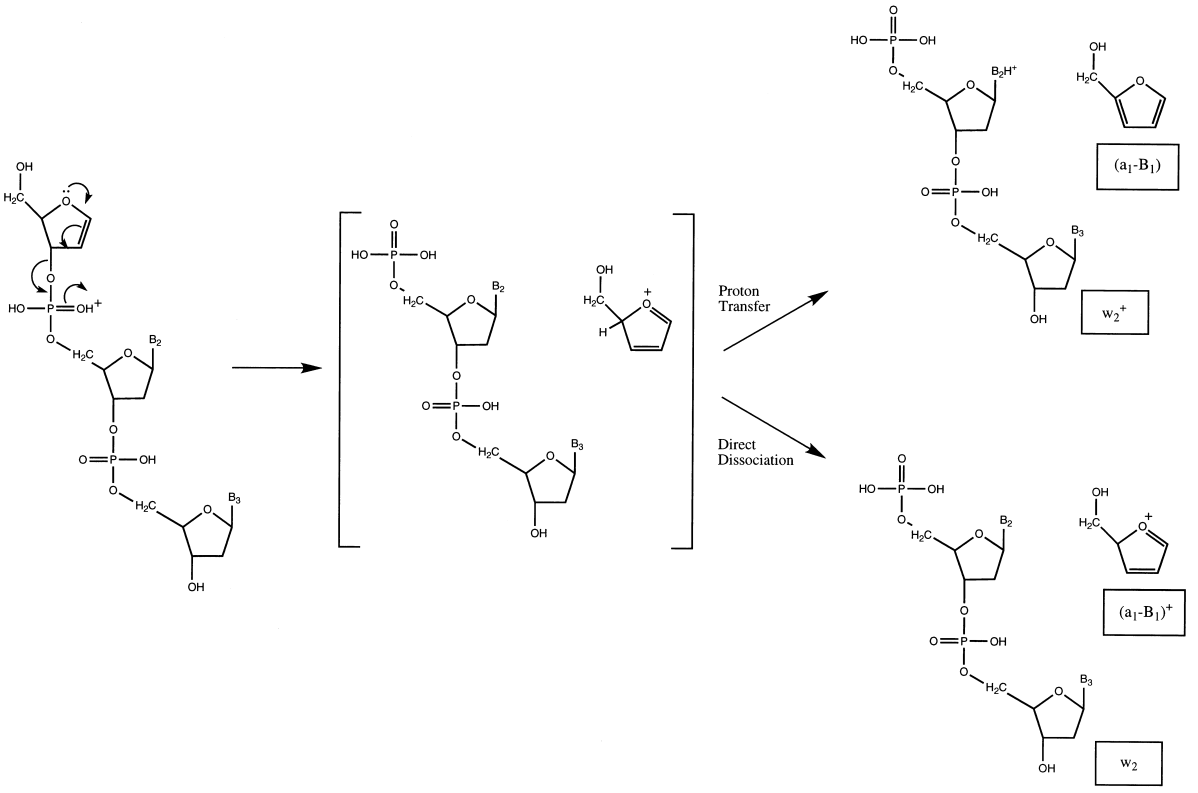

Scheme 5.

quence ions used here [9] should formally be labelled $(a_n - B_nH)^+$ to reflect the loss of the base plus a proton. In addition, the singly charged w ions should also be denoted $(w_n + nH)^{n+}$ to reflect the fact that the masses of these ions correspond to the cleavages shown in Scheme 1.

These sequence ions can be formed via two processes: (i) direct fragmentation of the $[M + H]^+$ ion, and (ii) from the "non-sequence" $[M + H - B_nH]^+$ ions, whereby cleavage of the 3′ − C–O phosphodiester bond yields an ion-molecule complex, in which the charged and neutral species are held together by electrostatic forces (Scheme 5). Note that Beauchamp has postulated that related ion-molecule complexes play an important role in the fragmentation reactions of $[M + H]^+$ ions of dideoxynucleotides [10]. If the lifetime of the ion-molecule complex is long enough, subsequent reactions leading to formation of either w- or (a − B)-type ions could occur via mechanisms involving either proton transfer or direct dissociation, respectively. One of the driving forces behind formation of the w_2^+ ion, typically observed in relatively high abundance for the trimer oligodeoxynucleotides studied here, may be the creation of the stable aromatic neutral $(a_1 - B_1)$ furan ring. Additionally, the relative proton affinity of the w_2-type fragment would be expected to be higher than the complementary furan due to the presence of the two remaining nucleic acid bases. The mechanism outlined above can also be applied to the loss of the second base (internal position), in which the w_1^+ and $(a_2 - B_2)^+$ sequence ions are formed. Fragmentation of the oxonium ion formed by base loss at the 3′ position via the E1 mechanism could result in the neutral loss of water and formation of an $(a_3 - B_3)^+$ product ion. Note that in each case, formation of the w- and (a − B) type sequence ions is dependent upon neutral base loss. The w_2^+ and $(a_1 - B_1)^+$ ions require 5′ (i.e. B_1) base

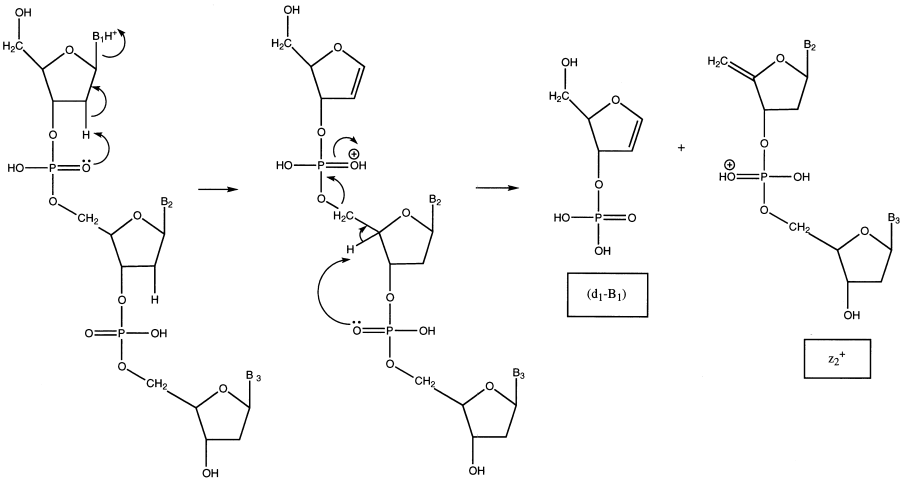

Scheme 6.

loss, w_1^+ and $(a_2 - B_2)^+$ ions require internal (i.e., B_2) base loss, and $(a_3 - B_3)^+$ ions require 3′ (i.e., B_3) base loss. In these studies, $(a_1 - B_1)^+$ ions were not observed, due to the inherent low mass range cutoff limitations associated with ion trap mass spectrometers.

Another ion that makes an appearance in a number of the spectra was the z_2^+ ion. The z_2^+ ion was observed in moderate abundances for oligodeoxynucleotides containing cytosine, guanine, and adenine at the 5′–terminus and in relatively high abundances when thymine was at the 5′–terminus (Table 1). The formation of the z_2^+ ion can occur via two distinct pathways. The first possible mechanism involves base loss from the 5′–terminus, followed by nucleophilic attack from the phosphate oxygen on the 3′ end to yield the z_2^+ ion and the $(d_1 - B_1)$ neutral (Scheme 6). This indirect formation of the z_2^+ ion occurs when cytosine, guanine, and adenine are present at the 5′–terminus. Since the nucleobases have a higher proton affinity than the phosphate group (Table 2), the charge is preferentially localized on the nucleobase. As a result, base loss must initially occur followed by cleavage of the C–O bond to form the z_2^+ ion and the $(d_1 - B_1)$ neutral. The second mechanism is possible when thymine is present at the 5′–terminus and when it is a thymine-rich species (e.g., TTT). Since thymine has such a low proton affinity, charge localization on the 5′–terminus phosphate oxygen becomes a viable alternative. Subsequent nucleophilic attack by the phosphate oxygen from the 3′–terminus results in direct formation of the the z_2^+ ion and the d_1 neutral (Scheme 7).

3.2. MS^3 studies on the $[M + H]^+$ ions of all 64 trimer oligodeoxynucleotides

To further investigate the origin and structural basis by which product ions formed by MS/MS undergo fragmentation, multistage tandem mass spectrometry (MS^3) in the quadrupole ion trap mass spectrometer was carried out. The prevailing reason for carrying out these studies was that in cases where complete sequence information was not available from the MS/MS spectra, MS^3 experiments could potentially provide further sequence information. In these studies, MS^3 experiments were restricted to an examination of the MS^3 spectra of each of the $[M + H - B_nH]^+$ "non sequence" and w_2^+ sequence ions, as these were generally the most abundant fragment ions observed in the MS/MS spectra.

In Tables 3–5, MS^3 data for the $[M + H - AH]^+$, $[M + H - GH]^+$, and $[M + H - CH]^+$ ions are reported. Initially, MS^3 experiments were carried out in cases where the position of the base loss could not be mistaken with any other (i.e. ACT, GCT, etc.). As

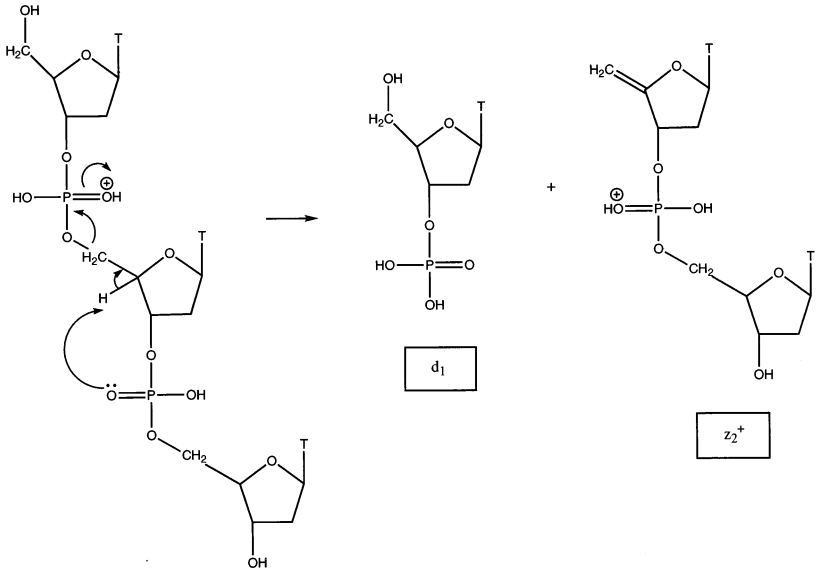

Scheme 7.

a result of the trends observed for these oligodeoxynucleotides, further work was carried out on the remaining oligodeoxynucleotides and correlations were made between the identity and position of the bases.

In accordance with the proposed mechanisms above, mass selection and fragmentation by CID of $[M + H - B_1H]^+$ ions resulted in formation of the w_2^+ ion as the major fragment (see Tables 3–5). In addition, some ions corresponding to further base loss, reliant upon the position and relative proton affinity of the base, also occurred. For example, MS^3 of the $[M + H - B_1H]^+$ (*m/z* 734.9) of d(ACG) from Fig. 1(A) resulted in the spectrum shown in Fig. 1(B) where the w_2^+ at *m/z* 636.8 was the major product ion observed.

In order to determine whether similar processes occur for fragmentation following base loss at either the 3′ or internal positions, MS^3 experiments were performed on each of the $[M + H - B_nH]^+$ ($n = 2$, 3) ions. MS^3 of the $[M + H - B_2H]^+$ ion from MS/MS of d(ACG) [Fig. 1(C)] yields a more complex spectrum than that for the $[M + H - B_1H]^+$ ion, although the important sequence ions $(a_2 - B_2)^+$ (*m/z* 411.8) and w_1^+ (*m/z* 347.8) are observed. In addition to these sequence ions, other product ions included loss of adenine (*m/z* 623.8), which subsequently triggered the loss of a furan ring resulting in the $(w_2 - B_c)^+$ (*m/z* 525.8) ion, followed by loss of a phosphate group yielding the $(z_2 - B_c)^+$ (*m/z* 427.8) ion. Among the other product ions were loss of guanine (*m/z* 607.8), loss of water (*m/z* 740.7), and loss of guanine and water (*m/z* 589.9). Note that the appearance of the sequence ions $(a_2 - B_2)^+$ and w_1^+, which must form via processes analogous to the formation of the w_2^+ ion from MS^3 of the $[M + H - B_1H]^+$ ion (Scheme 5), was observed for each of the 64 trimer oligodeoxynucleotides studied (see Tables 3–5). Furthermore, the MS^3 experiments performed on $[M + H - B_2H]^+$ ions generally yielded a larger number of fragmentation products compared with the $[M + H - B_1H]^+$ and $[M + H - B_3H]^+$ ions.

MS^3 experiments performed on each of the $[M + H - B_3H]^+$ ions resulted in the major neutral loss of water with formation of an $(a_3 - B_3)^+$ type ion (see Tables 3–5). A possible mechanism is shown in Scheme 8, whereby 3′ base loss via an E1 mechanism results in an intermediate which can subsequently undergo neutral water loss.

The final class of ion to be analysed via MS^3 experiments was the w_2^+ type sequence ion. In contrast to the $[M + H - B_nH]^+$ ions, where significant

Table 3
LCQ CID MS^3 of the $[M + H - AH]^+$ ions of the trimer oligonucleotides

		Product ions[a]					
		Sequence ions (% relative abundance)				Non-sequence ions (neutral loss, % relative abundance)	
Sample	$d(B_1B_2B_3)$	w_2^+	w_1^+	$(a_2 - B_2)^+$	$(a_3 - B_3)^+$	B_nH	B_nH_2O
1	AAA	100	3	5	27	B_AH, 13	B_AH_2O, 7
2	AAG	100	4	1	—	B_GH, 8; B_AH, 1	
4	AAT	100	—	6	—	B_AH, 1	
5	AGA	100	3	1	15	B_GH, 7; B_AH, 2	
6	AGG	100	1	—	—	B_GH, 7	B_GH_2O, 1
7	AGC	100	1	—	—	B_CH, 21; B_GH, 2	
8	AGT	100	1	—	—	B_GH, 2	
9	ACA	100	1	1	70	B_CH, 8; B_AH, 5	
10	ACG	100	—	—	—	B_CH, 6; B_GH, 2;	B_GH_2O, 4
11	ACC	100	—	—	—	B_CH, 49	B_CH_2O, 30
12	ACT	100	—	1	—	B_CH, 8; B_TH, 1	
13	ATA	100	—	—	45	B_AH, 1	
14	ATG	100	—	—	—	B_GH, 2	
33	CAA	—	2	—	100	B_CH, 12; B_AH, 1	B_CH_2O, 4; B_AH_2O, 1
41	CCA	—	—	2	100	B_CH, 7	
49	TAA	—	61	—	100	B_AH, 1	B_AH_2O, 2
52	TAT	—	7	19	—	B_TH, 12	B_TH_2O, 100
53	TGA	—	—	—	100		
57	TCA	—	—	—	100	B_CH, 3	B_CH_2O, 6

[a] Only those ions greater than or equal to 1% relative abundance are shown.

additional sequence information was obtained, MS^3 experiments on each of the w_2^+ type ions revealed base loss as the most abundant fragmentation process in all spectra (Table 6). The identity and abundance of the base loss was again dependent upon the relative proton affinities of the remaining bases and their position (i.e., in the order C ≈ G > A ≫ T and 3′ > internal position). Given that the major fragmentation process for the w_2 ions studied here involves the "non-sequence" ion neutral loss of base, MS^3 of small w-type ions is unlikely to be useful in providing additional structural information.

Note that in cases where following MS/MS, a base could be lost from multiple sites within the oligodeoxynucleotide (i.e., d(AAA), d(ACA), etc.) a mixture of product ions was observed upon MS^3, which can complicate the interpretation of these spectra.

3.3. MS/MS and MS^3 studies on the $[M + H]^+$ ions of 16 tetramer oligodeoxynucleotides

To determine whether the trends that appeared in the MS/MS and MS^3 spectra of the trimer oligodeoxynucleotides could be applied to slightly larger systems, tandem mass spectrometric experiments were performed on the $[M + H]^+$ ions of 16 tetramer oligodeoxynucleotides each containing A, T, G, and C (Table 7). Fig. 2 [i.e. d(AGCT)] shows a typical example of the type of MS/MS spectra obtained for the majority of samples. Abundant product ions cor-

Table 4
LCQ CID MS^3 of the $[M + H - GH]^+$ ions of the trimer oligonucleotides

		Product ions[a]					
		Sequence ions (% relative abundance)				Non-sequence ions (neutral loss, % relative abundance)	
Sample	d($B_1B_2B_3$)	w_2^+	w_1^+	$(a_2 - B_2)^+$	$(a_3 - B_3)^+$	B_nH	B_nH_2O
2	AAG	—	—	4	100	B_AH, 20	B_AH$_2$O, 6
6	AGG	—	13	26	100	B_GH, 25; B_AH, 25	B_GH$_2$O, 11
8	AGT	—	—	100	—	B_AH, 6	
10	ACG	—	—	2	100	B_CH, 3; B_AH, 2	
14	ATG	—	—	—	100	B_AH, 1	
17	GAA	100	1	—	—	B_AH, 2	B_AH$_2$O, 1
18	GAG	100	—	—	4		
19	GAC	100	—	—	1	B_CH, 19	B_CH$_2$O, 3
20	GAT	100	—	—	1		
21	GGA	100	4	1	—	B_GH, 8; B_AH, 1	
22	GGG	100	1	1	2	B_GH, 8	
23	GGC	100	1	1	—	B_CH, 19; B_GH, 2	B_CH$_2$O, 1
24	GGT	100	—	4	—	B_GH, 1; B_TH, 1	
25	GCA	100	1	—	—	B_CH, 5; B_AH, 1	B_AH$_2$O, 2
26	GCG	100	1	—	8	B_CH, 6; B_GH, 3	B_GH$_2$O, 4
27	GCC	100	—	—	—	B_CH, 64	
28	GCT	100	1	—	1	B_CH, 6	
29	GTA	100	1	—	—	B_AH, 1	
30	GTG	100	—	—	9	B_GH, 1	B_GH$_2$O, 1
31	GTC	100	—	—	—	B_CH, 14	B_CH$_2$O, 3
34	CAG	—	—	1	100	B_CH, 10	B_CH$_2$O, 7
38	CGG	—	3	4	86	B_CH, 100; B_GH, 17	B_CH$_2$O, 20
39	CGC	—	—	57	—	B_CH, 80	
42	CCG	—	—	1	100	B_CH, 13	B_CH$_2$O, 10
46	CTG	—	—	—	100	B_CH, 24	
50	TAG	—	—	—	100	—	B_AH$_2$O, 1
53	TGA	—	100	—	—		B_AH$_2$O, 2
54	TGG	—	100	—	83	B_GH, 2	B_GH$_2$O, 7
55	TGC	—	73	1	100	B_CH, 7	B_CH$_2$O, 21
56	TGT	—	—	29	—		B_TH$_2$O, 100
58	TCG	—	—	—	100		B_CH$_2$O, 2

[a] Only those ions greater than or equal to 1% relative abundance are shown.

responding to the loss of the neutral bases, adenine (*m/z* 1039.2), guanine (*m/z* 1023.1), cytosine (*m/z* 1063.1) and w_3^+, w_2^+, $(a_3 - B_3)^+$, and $(a_2 - B_2)^+$ ions (*m/z* 941.1, 612.0, 741.1, 412.0, respectively) were all observed. Following the trends proposed for the trimers oligodeoxynucleotides, we were able to predict that loss of the 5′ base (adenine) would produce w_3^+ ions, loss of the second base (guanine) would yield the w_2^+ and $(a_2 - B_2)^+$ ions, and loss of the third base (cytosine) would yield the w_1^+ and $(a_3 - B_3)^+$ ions. Subsequent MS^3 experiments on each of the "nonsequence" neutral base loss product ions confirmed these predictions (data not shown).

In addition to forming singly charged ions, the tetrameric oligodeoxynucleotides were also observed, under the ionization conditions employed, to form doubly charged ions (i.e. $[M + 2H]^{2+}$). Due to coulombic repulsion, the two charges are likely to be localised on the first and fourth nucleobases, making them good leaving groups, suggesting that the fragmentation of these may be similar to that of the singly charged ions, where the 3′ and 5′ bases were shown to

Table 5
LCQ CID MS^3 of the $[M + H - CH]^+$ ions of the trimer oligonucleotides

		Product ions[a]					
		Sequence ions (% relative abundance)				Non-sequence ions (neutral loss, % relative abundance)	
Sample	$d(B_1B_2B_3)$	w_2^+	w_1^+	$(a_2 - B_2)^+$	$(a_3 - B_3)^+$	B_nH	B_nH_2O
3	AAC		—	4	100	B_AH, 21	B_AH_2O, 8
7	AGC	—	—	2	100	B_AH, 3; B_GH, 2	
9	ACA	—	86	65	—	B_AH, 100	B_AH_2O, 11
10	ACG	—	42	86	20	B_GH, 100; B_AH, 64	
11	ACC	—	—	1	100	B_CH, 3; B_AH, 1	B_CH_2O, 3; B_AH_2O, 1
12	ACT	—	1	100	—	B_AH, 3	B_AH_2O, 1
15	ATC	—	—	—	100	B_AH, 1	
19	GAC	—	—	—	100	B_GH, 76	B_GH_2O, 13
23	GGC	—	—	—	100	B_GH, 73	B_GH_2O, 21
25	GCA	—	17	27	—	B_AH, 9; B_GH, 100	
26	GCG	—	11	23	—	B_GH, 100	B_GH_2O, 6
27	GCC	—	—	—	100	B_GH, 21; B_CH, 9	
28	GCT	—	2	100	—	B_GH, 7	
31	GTC	—	—	—	100	B_GH, 15	B_GH_2O, 3
33	CAA	100	1	—	—	B_AH, 2	
34	CAG	100	1	—	—	B_GH, 4	
35	CAC	70	—	—	100	B_CH, 35; B_AH, 1	B_CH_2O, 11; B_AH_2O, 1
36	CAT	100	—	—	—		
37	CGA	100	2	—	—	B_GH, 7; B_AH, 1	
38	CGG	100	1	—	—	B_GH, 4	B_GH_2O, 1
39	CGC	100	1	1	15	B_CH, 24; B_GH, 3	
40	CGT	100	—	—	—	B_GH, 2	
41	CCA	100	43	11	—	B_CH, 68; B_AH, 7	
42	CCG	100	11	4	—	B_CH, 46; B_GH, 14	
43	CCC	42	1	11	100	B_CH, 60	B_CH_2O, 34
44	CCT	100	1	11	—	B_CH, 22	B_CH_2O, 1
45	CTA	100	1	—	—	B_AH, 1	
46	CTG	100	—	—	—	B_GH, 2	B_GH_2O, 1
47	CTC	100	—	—	43	B_CH, 21	
51	TAC	—	—	—	100		
55	TGC	—	—	1	100	B_GH, 1; B_TH, 1	B_GH_2O, 1
57	TCA	—	100	—	—	B_TH, 1; B_AH, 1	B_AH_2O, 2
58	TCG	—	100	—	—	B_GH, 7; B_TH, 1	
59	TCC	1	2	—	100		
60	TCT	—	19	82	—	B_TH, 11	B_TH_2O, 90

[a] Only those ions greater than or equal to 1% relative abundance are shown.

be the most labile. Indeed, the spectra obtained from MS/MS experiments on the $[M + 2H]^{2+}$ ions (Table 8) were very similar to those of the $[M + H]^+$ ions described above (compare Table 8 to Table 7). Note that charged base loss dominates (with concomitant formation of singly charged $[M + 2H - B_nH_2]^+$ product ions), and that neutral base loss (with formation of $[M + 2H - B_nH]^{2+}$ product ions) is a very minor process. This provides further indirect evidence for the formation of ion-molecule complexes, where the neutral base initially lost reacts via proton transfer (c.f. Scheme 2). Additionally, the MS^3 spectra on the singly charged fragmentation product ions produced from the doubly charged precursors were the same as

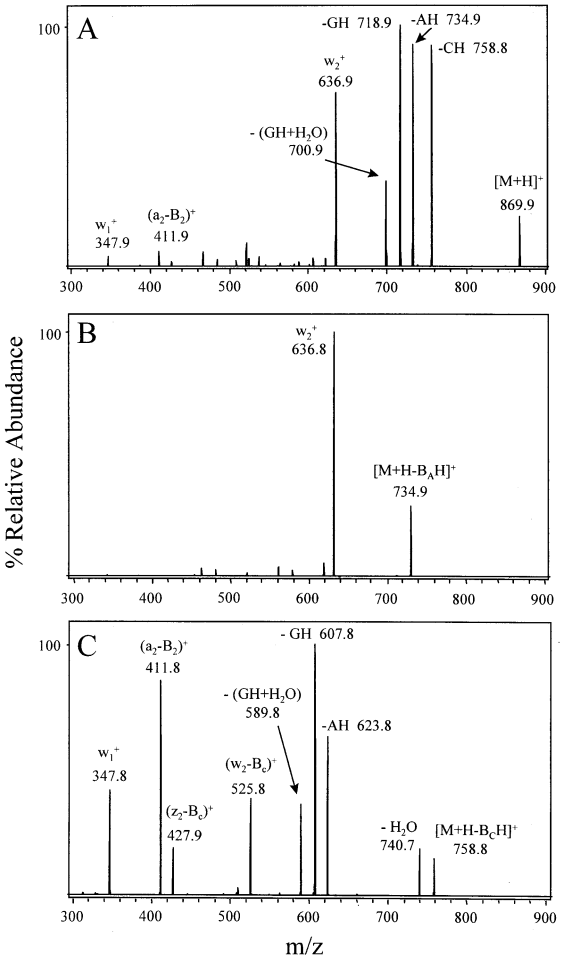

Fig. 1. (A) MS/MS of the $[M + H]^+$ ion of the protonated trimer oligodeoxynucleotide d(ACG). MS^3 spectra of (B) the $[M + H - B_1H]^+$ ion and (C) the $[M + H - B_2H]^+$ ion of d(ACG).

those from the singly charged precursors (data not shown).

Taken together, these results suggest that the general rules proposed for the fragmentation of the singly charged protonated trimer oligodeoxynucleotide ions can be applied to larger systems and to the fragmentation of multiply charged precursor ions. Note, however, that the trends for neutral nucleobase loss from $[M + H]^+$ and charged nucleobase loss from $[M + 2H]^{2+}$ are complicated. For $[M + H]^+$ ions: (i) 5′ base loss is generally favoured over other positions except for T, (ii) 3′ base loss is a minor process except for C, (iii) base loss from internal positions is only a significant process for G and C. For $[M + 2H]^{2+}$ ions, 5′ and 3′ base loss (charged) is preferred over internal base loss (charged). Generally, charged or neutral T loss is a minor or nonexistent process, the only exception being for GATC.

How do our results compare to two previous studies on tetramer and larger oligodeoxynucleotides, which were carried out using triple quadrupole mass spectrometers [12,13]? In direct correlation with the results obtained by these workers, the MS/MS spectra of the $[M + 2H]^{2+}$ ions for CGTA, AGTC, and ACGT in the ion trap show the presence of both the w- and (a − B)-type ions. One major difference, however, is due to charged base loss which should yield the pair of ions $[BH]^+$ and $[M + 2H - BH]^+$. In our ion trap studies only the $[M + 2H - BH]^+$ ions were observed, while in the triple quadrupole studies the $[BH]^+$ ions dominated. Whether this is due to the multiple collision conditions in the triple quadrupole instruments which may provide secondary pathways to the $[BH]^+$ ions from other fragment ions, or whether it is due to the low mass range limitations of the ion trap, is unclear.

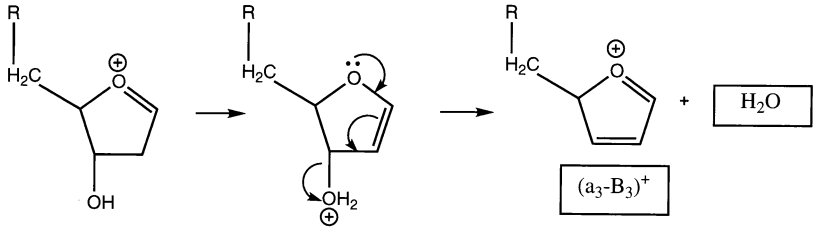

Scheme 8.

Table 6
LCQ CID MS^3 of the w_2^+ ions of the trimer oligonucleotides

Sample w_1^+	$d(B_1B_2B_3)$	Product ions[a]			
		Sequence ions (% relative abundance)		Non-sequence ions (neutral loss, % relative abundance)	
		w_1^+	$(a_2 - B_2)^+$	B_nH	B_nH_2O
1	AAA	40	—	B_AH, 100	B_AH_2O, 99
2	AAG	3	1	B_GH, 100; B_AH, 17	B_GH_2O, 76
4	AAT	7	—	B_AH, 15; B_TH, 11	B_TH_2O, 9
5	AGA	44	1	B_GH, 100; B_AH, 72	
6	AGG	12	—	B_GH, 100	B_GH_2O, 3
7	AGC	5	—	B_CH, 100; B_GH, 15	B_CH_2O, 28
8	AGT	—	—	B_GH, 66	
9	ACA	24	—	B_CH, 100; B_AH, 17	B_AH_2O, 71
10	ACG	14	—	B_CH, 76; B_GH, 43	B_GH_2O, 100
12	ACT	1	—	B_CH, 58; B_TH, 2	B_TH_2O, 3
13	ATA	3	—	B_AH, 2; B_TH, 2	B_AH_2O, 100; H_2O, 2
14	ATG	1	—	B_GH, 18	B_GH_2O, 100
16	ATT	—	—	B_TH, 7	
17	GAA	43	—	B_AH, 100	B_AH_2O, 96
18	GAG	—	—	B_GH, 100; B_AH, 17	
19	GAC	—	—	B_CH, 100; B_AH, 3	B_CH_2O, 38
20	GAT	6	—	B_AH, 16; B_TH, 3	
21	GGA	53	—	B_GH, 100; B_AH, 82	
22	GGG	—	—	B_GH, 100	
23	GGC	3	—	B_CH, 100; B_GH, 14	B_CH_2O, 19; B_GH_2O, 1
24	GGT	—	—	B_GH, 57	
25	GCA	30	—	B_CH, 100; B_AH, 23	B_AH_2O, 81
26	GCG	9	—	B_CH, 81; B_GH, 37	B_GH_2O, 100; B_CH_2O, 1
27	GCC	—	—	B_CH, 100	B_CH_2O, 51
28	GCT	1	—	B_CH, 48; B_TH, 1	
29	GTA	—	—	B_AH, 4	B_AH_2O, 100
30	GTG	—	—	B_GH, 4	B_GH_2O, 100
31	GTC	—	—	B_CH, 34	B_CH_2O, 100
32	GTT	—	—	B_TH, 4	B_TH_2O, 43
33	CAA	35	—	B_AH, 100	B_AH_2O, 89
34	CAG	3	—	B_GH, 100; B_AH, 14	
35	CAC	—	2	B_CH, 100; B_AH, 1	B_CH_2O, 48
36	CAT	14	—	B_AH, 12; B_TH, 9	B_TH_2O, 11
37	CGA	54	—	B_GH, 100; B_AH, 86	
38	CGG	6	—	B_GH, 100	
39	CGC	8	—	B_CH, 100; B_GH, 26	B_CH_2O, 33
40	CGT	1	—	B_GH, 57; B_TH, 1	
41	CCA	17	—	B_CH, 79; B_AH, 13	B_AH_2O, 100; B_CH_2O, 2
42	CCG	12	—	B_CH, 94; B_GH, 43	B_GH_2O, 100
43	CCC	—	2	B_CH, 100	B_CH_2O, 82
44	CCT	6	—	B_CH, 66	B_TH_2O, 3
45	CTA	11	—	B_AH, 6	
46	CTG	—	—	B_GH, 19; B_TH, 1	B_GH_2O, 100
47	CTC	—	—	B_CH, 89	B_CH_2O, 100
48	CTT	—	—	B_TH, 3	B_TH_2O, 57
49	TAA	20	—	B_AH, 32	B_AH_2O, 100
52	TAT	17	100	B_AH, 21	
64	TTT	—	16	B_TH, 31	B_TH_2O, 100

[a] Only those ions greater than or equal to 1% relative abundance are shown.

Table 7
LCQ CID MS/MS of the $[M + H]^+$ ions of the tetramer oligonucleotides

		Product ions[a] (% relative abundance)								
Sample	d($B_1B_2B_3B_4$)	−AH	−GH	−CH	−TH	w_3^+	w_2^+	$(a_4 - B_4)^+$	$(a_3 - B_3)^+$	$(a_2 - B_2)^+$
A	AGCT	100	69	67	—	76	76	—	52	5
B	GACT	—	70	6	5	100	—	—	—	—
C	GCAT	—	97	13	11	100	—	—	—	—
D	GCTA	—	100	12	7	75	—	—	—	—
E	ACGT	48	25	42	—	100	22	—	31	—
F	CAGT	8	13	48	—	100	—	—	15	—
G	CGAT	—	36	100	—	100	24	—	—	—
H	CGTA	6	12	69	—	100	5	—	—	—
I	AGTC	65	22	50	—	93	16	100	—	5
J	GATC	—	53	11	—	100	—	17	—	—
K	GTAC	—	100	17	—	98	—	29	—	—
L	GTCA	—	68	6	—	100	—	—	—	—
M	ATGC	50	33	68	—	100	—	92	31	—
N	TAGC	—	19	65	—	—	—	100	6	—
O	TGAC	10	59	66	—	—	62	100	—	—
P	TGCA	25	68	60	—	—	100	—	19	—

[a] Only those ions greater than or equal to 5% relative abundance are shown.

4. Conclusions

Electrospray ionization in conjunction with tandem mass spectrometry shows great promise as becoming a widespread oligodeoxynucleotide sequencing tool. We have demonstrated, using a combination of collisional activation in ion trap MS/MS and MS^3 experiments, the unequivocal assignment of all 64 trimer and 16 tetramer oligodeoxynucleotide sequences. Oligodeoxynucleotide sequencing is possible in the ion trap due to the following characteristic dissociation pathways:

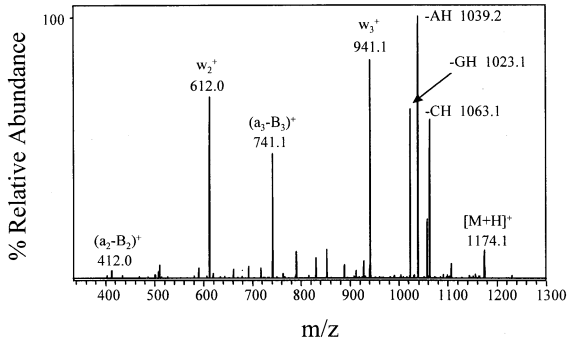

Fig. 2. MS/MS of the $[M + H]^+$ ion of the protonated tetramer oligodeoxynucleotide d(AGCT).

(a) The initial CID reaction mechanism for $[M + nH]^{n+}$ ions involves neutral base loss from the 5′ terminus when C and G are in that position, only sometimes when A is in that position (i.e. when C and G are not in the 3′ position), and not for T. The relative abundance of each of these neutral losses is dependent on the relative proton affinity, where C ≈ G > A ≫ T, and position within the oligodeoxyonucleotide sequence (5′ > 3′ > internal).
(b) Intramolecular proton transfer following base loss leads to cleavage of the 3′ − C–O phosphodiester bond (relative to the site of base loss) to yield an ion-molecule complex, which then undergoes either proton transfer or direct dissociation to yield complementary w- and (a − B)-type ions. For the trimer oligodeoxynucleotides, loss of the 5′ base yields w_2^+-type ions, loss of the 3′ base yields results in neutral water loss with formation of $(a_3 - B_3)^+$-type ions, and loss of the internal base yields w_1^+ and $(a_2 - B_2)^+$-type ions.
(c) In thymine-rich species (e.g. TTT), protonation at the phosphate oxygen becomes a viable process, which can result in the formation of the z_2^+ ion under CID conditions. Additionally, z_2^+ ion formation can

Table 8
LCQ CID MS/MS of the $[M + 2H]^{2+}$ ions of the tetramer oligonucleotides

		Product ions[a] (% relative abundance)													
Sample	$d(B_1B_2B_3B_4)$	$-(AH_2)^+$	$-(GH_2)^+$	$-(CH_2)^+$	$-(TH_2)^+$	$-AH$	$-GH$	$-CH$	$-TH$	w_3^+	w_2^+	w_1^+	$(a_4 - B_4)^+$	$(a_3 - B_3)^+$	$(a_2 - B_2)^+$
A	AGCT	25	19	100	—	—	—	—	—	18	18	—	—	74	17
B	GACT	6	100	7	—	—	—	—	—	67	—	—	—	—	—
C	GCAT	6	100	13	—	—	—	—	—	44	—	—	—	—	—
D	GCTA	24	100	47	—	—	—	—	—	56	12	—	—	—	7
E	ACGT	100	20	70	—	—	—	6	—	60	37	—	—	12	13
F	CAGT	11	—	100	—	—	—	—	—	32	—	—	—	—	—
G	CGAT	—	5	100	—	—	—	—	—	20	—	—	—	—	—
H	CGTA	33	—	94	—	—	—	—	—	100	—	—	36	—	—
I	AGTC	27	5	100	—	—	—	—	—	17	—	—	—	—	7
J	GATC	—	100	39	26	—	—	—	—	79	—	—	—	—	—
K	GTAC	—	100	37	—	—	—	—	—	34	—	—	—	—	—
L	GTCA	14	100	—	—	—	—	—	—	54	—	—	—	—	—
M	ATGC	53	—	100	—	—	—	—	12	23	—	—	—	—	—
N	TAGC	8	6	100	—	—	—	—	7	—	—	—	55	—	—
O	TGAC	11	16	100	—	—	—	—	5	—	16	—	58	—	—
P	TGCA	100	49	56	—	—	—	—	6	—	23	7	—	7	—

[a] Only those ions greater than or equal to 5% relative abundance are shown.

occur as a secondary process in a few cases where cytosine, guanine, or adenine are present at the 5′–terminus.

The proposed fragmentation reaction mechanisms for the 64 protonated oligodeoxynucleotides under low energy CID conditions revolves primarily around three key concepts: (i) the mechanisms are likely to be charge directed, (ii) in most instances, competing product ion formation can be rationalized as resulting from the intermediacy of an ion molecule complex which can either undergo proton transfer or direct dissociation (e.g. Schemes 2 and 5), and (iii) a labile proton could migrate via intramolecular proton transfer to potential cleavage sites. This latter concept is known as the mobile proton model [26,27] (where a labile proton is able, via intramolecular proton transfer, to migrate from one potential cleavage site to another to effect fragmentation) and has been applied to explaining the fragmentation mechanisms of protonated peptide systems. Taken together, these three factors are useful in rationalizing the fragmentation reactions observed in this study.

Supplementary material

Full MS/MS and MS^3 spectra are available from the corresponding author.

Acknowledgements

R.A.J.O. thanks the ARC (Grant No. A29930202) for financial support and the University of Melbourne for funds to purchase the LCQ. G.E.R. acknowledges the award of a Commonwealth Postgraduate Scholarship. We would like to thank Dr. Tony Hodder for access to the HPLC used for oligodeoxynucleotide purification. The helpful comments of two reviewers are also acknowledged.

References

[1] D.C. Muddiman, R.D. Smith, Rev. Anal. Chem. 17 (1998) 1.
[2] For reviews on the mass spectrometry of oligodeoxynucleotides see: (a) K.K. Murray, J. Mass Spectrom. 31 (1996) 1203; (b) E. Nordhoff, F. Kirpekar, P. Roepstorff, Mass Spectrom. Rev. 15 (1996) 67.

[3] A. Apfell, J.A. Chakel, S. Fischer, K. Lichtenwalter, W.S. Hancock, Anal. Chem. 69 (1997) 1320.
[4] D.A. Nickerson, V.O. Tobe, S.L. Taylor, Nucleic Acids Res. 25 (1997) 2745.
[5] S.A. Carr, M.E. Hemling, M.F. Bean, G.D. Roberts, Anal. Chem. 63 (1991) 2802.
[6] M.T. Rodgers, S. Campbell, E.M. Marzluff, J.L. Beauchamp, Int. J. Mass Spectrom. Ion Processes 137 (1994) 121.
[7] S.A. McLuckey, S. Habibi-Goudarzi, J. Am. Chem. Soc. 115 (1993) 12085.
[8] S.A. McLuckey, G. Vaidyanathan, S. Habibi-Goudarzi, J. Am. Chem. Soc. 30 (1995) 1222.
[9] S.A. McLuckey, G.J. van Berkel, G.L. Glish, J. Am. Soc. Mass Spectrom. 3 (1992) 60.
[10] M.T. Rodgers, S. Campbell, E.M. Marzluff, J.L. Beauchamp, Int. J. Mass Spectrom. Ion Processes 148 (1995) 1.
[11] J. Boschenok, M.M. Sheil, Rapid Commun. Mass Spectrom. 10 (1996) 144.
[12] P.P. Wang, M.G. Bartlett, L.B. Martin, Rapid Commun. Mass Spectrom. 11 (1997) 846.
[13] J. Ni, M.A.A. Matthews, J.A. McCloskey, Rapid Commun. Mass Spectrom. 11 (1997) 535.
[14] D.R. Phillips, J.A. McCloskey, Int. J. Mass Spectrom. Ion Processes 128 (1993) 61.
[15] (a) L. Grotjahn, R. Frank, H. Blocker, Nucl. Acids Res. 10 (1982) 4671. (b) L. Grotjahn, H. Blocker, R. Frank, Biomed. Mass Spectrom. 12 (1985) 514.
[16] (a) M. Greig, R.H. Griffey, Rapid Commun. Mass Spectrom. 9 (1995) 97. (b) R.P. Glover, G.M.A. Sweetman, P.B. Farmer, G.C.K. Roberts, Rapid Commun. Mass Spectrom. 9 (1995) 897.
[17] Base loss is a depurination reaction. For the only theoretical study to determine the dissociation energy see: D. Venkateswarlu, R.H.D. Lyngdoh, J. Mol. Struct. (Theochem) 418 (1997) 49.
[18] N. Russo, M. Toscano, A. Grand, F. Jolibois. J. Comp. Chem. 19 (1998) 989.
[19] J.E. Del Bene, J. Phys. Chem. 87 (1983) 367.
[20] E.P.L. Hunter, S.G. Lias, J. Phys. Chem. Ref. Data 27 (1998) 413.
[21] F. Greco, A. Liguori, G. Sindona, N. Uccella, J. Am. Chem. Soc. 112 (1990) 9092.
[22] T. Marino, V. Milano, N. Russo, M. Toscano, J. Mol. Struct. (Theochem) 306 (1994) 185.
[23] J. Smets, L. Houben, K. Schoone, G. Maes, L. Adamowicz, Chem. Phys. Lett. 262 (1996) 789.
[24] M.J. Scanlan, I.H. Hillier, J. Am. Chem. Soc. 106 (1984) 3737.
[25] M. Sabio, S. Topiol, W.C. Lumma Jr., J. Phys. Chem. 94 (1990) 1366.
[26] A.R. Dongre, J.L. Jones, A. Somogyi, V.H. Wysocki, J. Am. Chem. Soc. 118 (1996) 8365.
[27] A.G. Harrison, T. Yalcin, Int. J. Mass Spectrom. Ion Processes 165/166 (1997) 339.